

Simulation of Chemically Reacting Flow in Plasma Native Oxide Cleaning Process

Seung-Min Ryu

Dept. of Aerospace Engineering and
Engineering Mechanics
The University of Texas at Austin
Austin, U.S.
smryu@utexas.edu

Yunho Kim

Dept. of Aerospace Engineering and
Engineering Mechanics
The University of Texas at Austin
Austin, U.S.
ykim96@utexas.edu

Dylan Pederson

Dept. of Aerospace Engineering and
Engineering Mechanics
The University of Texas at Austin
Austin, U.S.
dpederson@utexas.edu

Jonghyun Lee

Memory Technology Innovation Team
Samsung Electronics
Hwaseong-si, South Korea

Youngkwon Kim

Memory Technology Innovation Team
Samsung Electronics
Hwaseong-si, South Korea

Laxminarayan L. Raja

Dept. of Aerospace Engineering and
Engineering Mechanics
The University of Texas at Austin
Austin, U.S.
lraja@mail.utexas.edu

Jiho Uh

Memory Technology Innovation Team
Samsung Electronics
Hwaseong-si, South Korea

Sang-Jin Choi

Memory Technology Innovation Team
Samsung Electronics
Hwaseong-si, South Korea

Abstract—A plasma native oxide cleaning process is widely used on the semiconductor production line to remove oxide impurities on silicon surfaces of a wafer. In this study, a flow simulation with microwave plasma species has been conducted to analyze the flow characteristics in a showerhead that affect the batch uniformity in the process. In particular, the distributions of temperature and mass flow rate of the gas as well as the number density of hydrogen radicals at the showerhead hole outlets were compared for different showerhead designs by using computational fluid dynamics. The distribution of gas temperature at the hole outlets was found to be inversely proportional to one of gas mass flow rate by the simulation results. However, mass flow rate distribution for the total gas shows a different trend from one of hydrogen radicals in the showerhead hole outlets. The showerhead design with low temperature gradient also showed a more uniform mass flow rate profile at the hole outlets, which was validated by the simulation results.

Keywords—Multi-physics, Simulation, Plasma, Species, Flow

I. INTRODUCTION

A key issue for semiconductor manufacturing plants is to increase the productivity and yield of high quality chips simultaneously [1]. Semiconductor companies have tried to obtain better uniformity of the pattern features as well as the electrical characteristics of the wafer. Specifically, a Si thermal deposition process is one of the most challenging areas in the semiconductor fabrication because it is difficult to achieve pattern uniformity due to a narrow range of acceptable process parameters and sensitivity to pre-cleaned surface conditions. For instance, the Si layer is deposited uniformly on the super-clean Si surface of the wafer, especially in the Si epitaxial growth process, but the oxygen atoms on the Si surface interfere with the growth of the Si layer, which results in nonuniform pattern height. To resolve this issue, it has become critical to effectively remove the oxide layer from the Si wafer for the advanced devices, which has motivated the semiconductor industry to optimize various native oxide removal methods to obtain high performance of the devices. As a chemical dry cleaning process, batch type plasma native oxide cleaning (PNC) equipment has been widely used to treat

and remove a native oxide layer on the Si surface due to its high throughput and superior cleaning efficiency. However, it has been difficult to obtain even distribution of gas temperature as well as species concentration in the batch chamber. The key requirement of the process is to make the silicon surface ultra clean uniformly across the wafers in the batch chamber [2].

In this paper, firstly we study the flow mechanism by computational fluid dynamic (CFD) simulation to elucidate potential causes related to the batch uniformity. Then we analyze characteristics of gas flow in a different showerhead design affecting uniform cleaning quality in the PNC equipment.

II. BACKGROUND AND NUMERICAL PROCEDURE

A. PNC process

The schematic of a batch-type PNC equipment is as shown in Fig. 1. There are two types of gas inlet ports in the chamber. A mixture of N_2 and NH_3 gas enters the two applicators and is dissociated by a continuous wave source driven at 2.45 GHz. Hydrogen radicals are generated in the applicator and supplied to the process chamber through a showerhead inlet. An NF_3 gas directly enters the chamber through straight nozzles. Production and dummy wafers are loaded together on a wafer-boat in the vertical type chamber at one time. The exhaust port is located in the center of the chamber opposite to showerhead and the outlet pressure of the chamber is controlled by automatic pressure valve. Halogen lamps are installed to heat the wafers to vaporize and remove the by-product on the wafers after the etch step.

B. Simulation procedure

The simulation consists of three different parts. First, the plasma discharge is simulated to obtain the mole fractions of plasma generated species inside a microwave waveguide applicator. Second, a steady-state fluid flow simulation is performed for each test case to obtain the distribution of pressure, temperature and mass flow rates at the hole outlets of the showerhead. Finally, reacting flow simulations are conducted with the inclusion of the neutral plasma generated

species. The main goal of these simulations is to obtain the transport characteristics of the plasma generated radical species to the showerhead hole outlets of the gas. For this study, reactive hydrogen radicals are of main interest as they become an important source for the formation of etchants ($NH_x F_y$) [3-6].

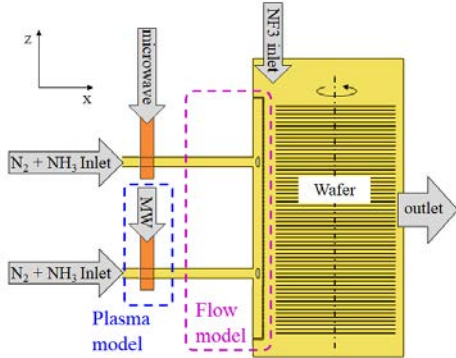


Fig. 1. Chamber structure for PNC batch process.

C. Plasma and reacting flow chemistry

For the simulation of plasma discharge, a kinetic mechanism that includes 23 Species and 152 reactions is used. The database is provided by VizGlow [7]. The species include: e , NH_3 , NH_3^+ , NH_4^+ , NH_2 , NH_2^+ , NH_2^- , NH , NH^+ , N , NH^+ , N , N^+ , N_2 , N_2^+ , H , H^+ , H^- , H_2 , H_2^+ , H_3^+ , N_2H_2 , N_2H_3 , N_2H_4 , $NH_3(v)$. For the reacting flow simulation, all charged species and reactions that involve them are ignored. This assumption is reasonable since the recombination of charged species occurs in μs timescale or less, which is much smaller than the flow timescale (ms). To model the loss of atomic hydrogen during its transport to the outlet holes, the surface recombination coefficient is set as 0.01 [8].

D. Microwave plasma simulation

a) *Microwave plasma discharge*: Plasma discharge simulation is performed to obtain the mole fraction of each species generated by the plasmas. The mole fractions are used as the inlet boundary condition of the reacting flow simulation in the next section. Based on the pressure and temperature at the inlet of the showerhead obtained from the fluid flow simulation, a plasma discharge simulation is conducted to find out the species number densities at quasi-steady state. At a fixed mass flow rate of $2.0 \times 10^{-4} kg/s$ and the temperature of $700K$, the inlet pressures are $300Pa$ and $600Pa$ for the Case I and Case II, respectively. These temperature and pressures are chosen as the operating conditions of an NH_3/N_2 mixture. Numerical models developed for high frequency plasma discharges are used for this section [9-10].

b) *Computational domain*: To model the microwave discharge, a downstream plasma source built by MKS is considered [11]. It employs the TE_{10} mode of a rectangular waveguide whose side view of the schematic is shown in Fig. 2. In the figure, D (25mm) is the diameter of the quartz tube, L (30.6mm) is the distance between the tube and the short plunger at the end of the waveguide, and H (33mm) is the height of the waveguide. L is the quarter wavelength of the operating frequency (2.45GHz) which indicates the standing wave formation inside. The maximum wave amplitude occurs

near the surface of the dielectric shown as the thin grey area in Fig. 2. The dielectric quartz thickness is 2mm and its relative dielectric permittivity is 3.8. We model the electromagnetic wave propagation as a simple 1D waveguide as shown in the Fig. 2 by impinging the plane wave from the left. The Perfectly Matched Layer (PML) is implemented on the left to effectively absorb the reflected waves from the short plunger. While the Maxwell's equations are solved in the entire computational domain, the self-consistent plasma governing equations are solved only inside the plasma subdomain.

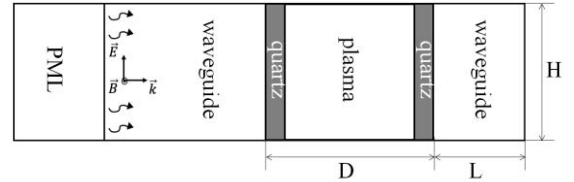


Fig. 2. Schematic of the 1D waveguide.

E. Reacting flow simulation

Two showerhead designs were modeled to check the distribution of mass flow rate including radical species and gas temperature in the hole outlets of the showerhead. The simulation consists of a two-step process. First, steady state 2D analysis of the gas flow inside the showerhead was conducted using only the fluid flow solver in VizGlow. The models were meshed with dominant quadrilateral and triangular elements. The total mass flow rate of the process gases was used as an inlet condition of the model. The gases were assumed to be ideal gas. Major boundary conditions for the models are shown in Table 1. The temperature at the gas inlet was set as $700K$. The static pressure $200 Pa$ was set as outlet boundary condition of the chamber. The constant temperature on the backside surface of the showerhead is applied to the wall condition because the chamber wall in contact with the showerhead is cooled and kept at $300K$ during the process. The other surfaces of the showerhead were assumed to have thermally insulated walls. Then, a transient simulation of the gas flow including radical species generated by microwave plasma in the applicator was conducted using a species density solver in VizGlow. In particular, the species density solver includes bulk chemical reactions as well as surface reactions on the wall. The time step was set to $1.0 \times 10^{-6}s$ to resolve the chemical reaction timescale. Two types of showerhead design with different gas flow paths are shown in Fig. 3. Especially, mass flow rate, temperature and the number density of the hydrogen radical species were monitored at the hole outlets of the showerhead.

TABLE I. BOUNDARY CONDITIONS FOR GAS FLOW SIMULATION MODEL

Process parameter	Mass flow rate at inlet(kg/sec)		Pressure at the outlet(Pa)	Wall conditions	
	N_2	NH_3		Showerhead backside surface	Other surfaces
value	1.63×10^{-4}	3.29×10^{-5}	200	300K Constant Temp.	Thermally Insulated

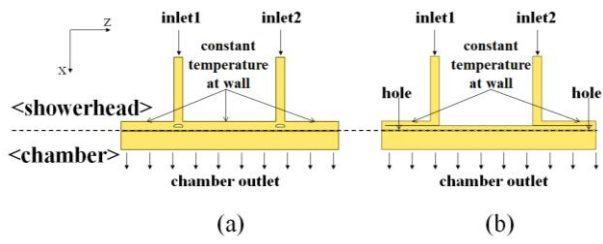


Fig. 3. Showerhead designs of (a) Case I and (b) Case II.

III. RESULT AND DISCUSSION

A. Microwave plasma formation

At each operating pressure, the ratio of the seed number densities of NH_3 and N_2 is given as 1:3 according to the inlet flow condition, respectively. The order of magnitude of the number densities are $10^{22}m^{-3}$. For all other species, the seed number density is set as $10^{12}m^{-3}$. The incident wave amplitude is set as $50kV/m$. The transient plasma formation is shown in Fig. 4 where the tracepoint is $2.5mm$ away from the dielectric surface on the right. Here, the generation of radical species H , NH , and NH_2 is important as they mainly participate in the formation of etchants (NH_xF_y) [3]. The order of magnitude of these species densities is comparable to or larger than the electron number density ($10^{18}m^{-3}$). The mole fraction of each species is obtained from these results. For the operating pressure of $300Pa$, the mole fractions of H , NH , and NH_2 are found to be 1.98×10^{-4} , 4.07×10^{-5} and 1.30×10^{-4} , respectively. For $600Pa$, they are 1.93×10^{-4} , 3.38×10^{-5} , and 1.39×10^{-4} , respectively. The mole fractions of the other neutral species are also obtained and used as the inlet boundary condition for the reacting flow simulation in the next section.

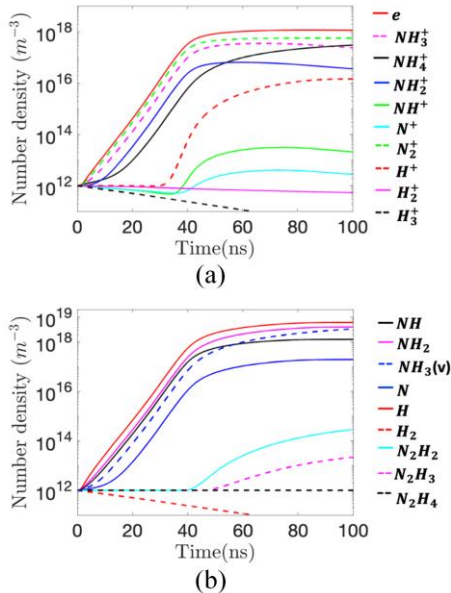


Fig. 4. Transient evolution of species number density. (a) Charged species and (b) neutral species.

B. Fluid characteristics in the showerhead

Case I shown in Fig. 5(a) has diffusers to disperse the gas throughout the showerhead and obtain flow uniformity in the

showerhead. However, Case II without any diffuser in Fig. 5(b) has returning paths of the gas at both sides to maintain continuous flow in the showerhead. Inlet pressure values of Case I and Case II model used in the microwave plasma simulation were calculated by the CFD models to be $300Pa$ and $600Pa$, respectively, as shown in Fig. 5. Return paths of gas flow in the Case II made pressure drop larger in the showerhead, whose inlet pressure is about twice larger than Case I. The pressure inside both chambers were nearly $200Pa$ which is similar to the outlet boundary condition.

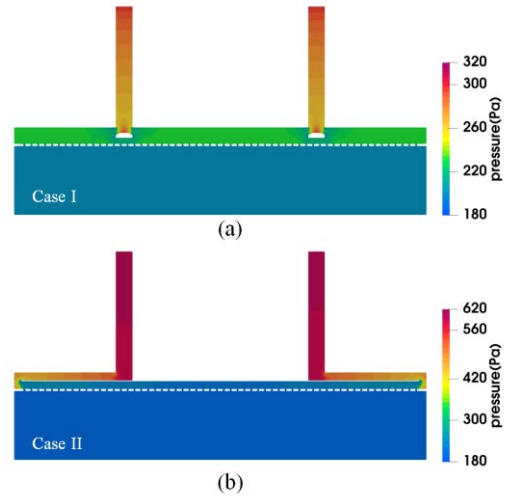


Fig. 5. Pressure distribution of showerhead models; (a) Case I and (b) Case II.

The distribution of temperature normalized by inlet gas temperature $700K$ at each hole of the showerhead is plotted in Fig. 6. The gas temperature in Case I gradually decreases with distance from the applicators because of conductive heat loss from the showerhead to the chamber. Therefore, the temperature distribution of the gas in the showerhead shows an 'M'-shaped profile as shown in Fig. 6. Case II exhibits relatively flat shape in the temperature profile compared to Case I. Case II shown in the Fig. 6, however, has no diffusers but instead there is a thermally isolated vacuum barrier to change the gas flow path and prevent heat flux from the showerhead to process chamber. Here it is important to reduce the heat flux from the hot gas to the chamber through the showerhead. The temperature distribution of the gas at the hole outlets of the showerhead was affected by the showerhead backside area in contact with the chamber.

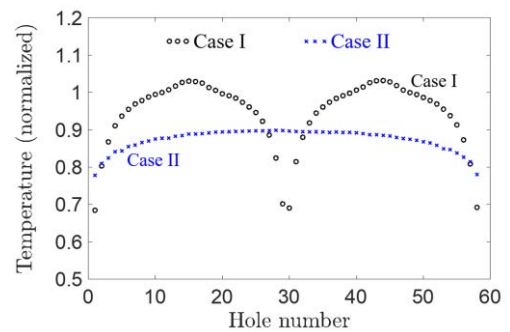


Fig. 6. Normalized temperature distribution at the hole outlets of the showerheads.

The distributions of total gas mass flow rate and number density for hydrogen radicals normalized by inlet flow condition for each showerhead design are shown in Fig. 7 and Fig. 8, respectively. It is found on the distribution that the mass flow rate is inversely dependent on the gas temperature. For both models, the distribution of hydrogen radicals has a different trend compared to the mass flow rate. It is noticeable that it depends on the flow path. Case II shows 16% and 23% better uniformity in the process zone than Case I in terms of the number density of hydrogen radical species and temperature, respectively. However, the radical species loss in Case I is smaller than Case II due to its shorter flow path which yields less amount of surface recombination. The simulation results imply that Case II can show the better the etch rate uniformity but lower silicon oxide etch amount on the wafer.

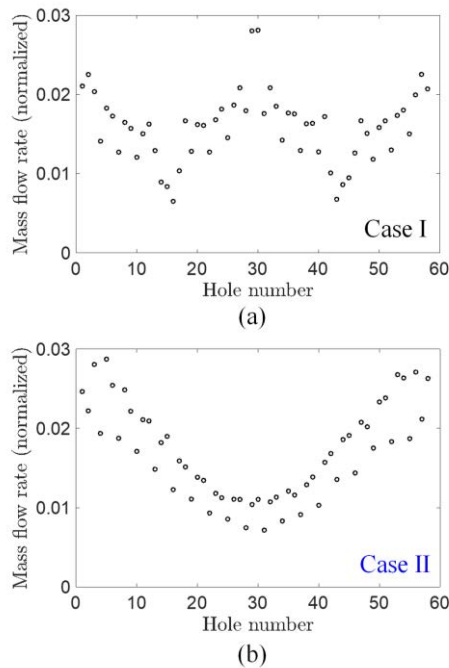


Fig. 7. Distribution of normalized mass flow rates at the hole outlets of the showerheads; (a) Case I and (b) Case II.

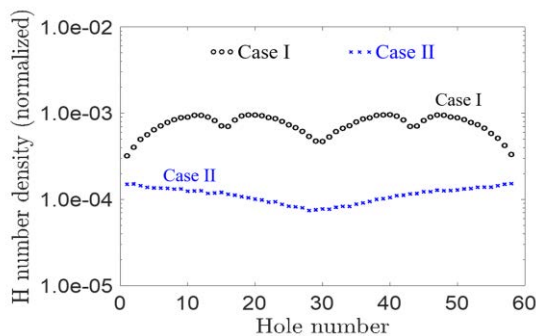


Fig. 8. Distribution of normalized number densities for hydrogen radical species at the hole outlets of the showerheads.

IV. CONCLUSIONS

The effects of showerhead design on flow characteristics are studied in this work to estimate their correlation to the process uniformity. High frequency plasma discharge model

and chemically reacting flow model are employed to find out the distribution of temperature and plasma generated radical species. Mass flow rate at the hole outlets of the showerheads was inversely dependent on the gas temperature, which is affected by the heat flux to the showerhead backside surface. However, the distribution of number density for hydrogen radicals was affected by the flow path of the gas in the showerhead. By altering the flow path, the gas temperature gradient at the hole outlets was changed to yield better uniformity. CFD simulation results show the showerhead design with a vacuum barrier has 23 % lower temperature gradient in the process zone than without the thermal barrier. It is also shown that the showerhead with the thermally isolated barrier had improved 16% in hydrogen radical flow uniformity. However, the radical species loss was larger for the case with a longer flow path.

ACKNOWLEDGMENT

This work was supported by Samsung Electronics Co., Ltd.

REFERENCES

- [1] K. Kim, "Silicon technologies and solutions for the data-driven world", IEEE International Solid-State Circuits Conference, 2015, pp. 8-14.
- [2] W. S. Kim, W. G. Hwang, I. Kim, K. Yun, K. M. Lee and S. K. Chae, "Development of New Batch-Type Plasma Assisted NOR (Native-Oxide-Removal) Dry Cleaning Equipment", Solid State Phenomena, 2005, pp. 63-66, vol. 103-104.
- [3] T. Hayashi, Recent Development of Si Chemical Dry Etching Technologies", J. of Nanomedicine & Nanotechnology, 2012, s15:001.
- [4] N. Posseme, V. Ah-Leung, O. Pollet, C. Arvet and M. Garcia-Barros, "Thin layer etching of silicon nitride: A comprehensive study of selective removal using NH₃/NF₃ remote plasma", J. Vac. Sci. Technol. A, 2016, vol. 34, no. 6, pp. 061301.
- [5] H. Nishino, N. Hayasaka, and H. Okano, "Damage - free selective etching of Si native oxides using NH₃/NF₃ and SF₆/H₂O down - flow etching", 1993, J. Appl. Phys., vol. 74, no. 2, pp.1345-1348.
- [6] H. J. Oh, J. H. Lee, M. S. Lee, W. G. Shin, S. Y. Kang, G. D. Kim and D. H. Ko, "NF₃/NH₃ Dry Cleaning Mechanism Inspired by Chemical and Physical Surface Modification of Si, SiO₂, and Si₃N₄", ECS Transactions, 2014, vol. 61, pp. 1-8.
- [7] <https://esgeetech.com/>
- [8] B. J. Wood and H. Wise, " the Kinetics of Hydrogen Atom Recombination on Pyrex Glass and Fused Quartz 1 ," J. Phys. Chem., 2007, vol. 66, no. 6, pp. 1049-1053.
- [9] P. P. Chelvam and L. L. Raja, "Modeling of gas breakdown and early transients of plasma evolution in cylindrical all-dielectric resonators," J. Phys. D. Appl. Phys., 2017, vol. 50, no. 47.
- [10] Y. Kim and L. L. Raja, "Modeling of microwave surface plasmas on the meta-surface at atmospheric pressure," in AIAA Scitech 2019 Forum, 2019, no. January, pp. 1-13.
- [11] M. Mehdizadeh. "Microwave/RF Applicators and Probes : for Material Heating, Sensing, and Plasma Generation", 2nd ed., Elsevier, 2015, pp. 348-351.